

Formal selection rules for Brillouin scattering in integrated waveguides and structured fibers

C. Wolff,^{1,2,*} M. J. Steel,^{1,3} and C. G. Poulton^{1,2}

¹ Centre for Ultrahigh Bandwidth Devices for Optical Systems (CUDOS), Australia

² School of Mathematical Sciences, University of Technology Sydney, NSW 2007, Australia

³ Department of Physics and Astronomy, Macquarie University Sydney, NSW 2109, Australia

[*christian.wolff@uts.edu.au](mailto:christian.wolff@uts.edu.au)

Abstract: We derive formal selection rules for Stimulated Brillouin Scattering (SBS) in structured waveguides. Using a group-theoretical approach, we show how the waveguide symmetry determines which optical and acoustic modes interact for both forward and backward SBS. We present a general framework for determining this interaction and give important examples for SBS in waveguides with rectangular, triangular and hexagonal symmetry. The important role played by degeneracy of the optical modes is illustrated. These selection rules are important for SBS-based device design and for a full understanding the physics of SBS in structured waveguides.

© 2014 Optical Society of America

OCIS codes: (190.5890) Nonlinear optics, scattering, stimulated; (130.4310) Integrated optics, Nonlinear.

References and links

1. R. W. Boyd, *Nonlinear optics* (Academic, 3rd edition, 2003).
2. L. Brillouin. "Diffusion de la lumière par un corps transparent homogène," *Annals of Physics* **17**, 88–122 (1922).
3. R. Y. Chiao, C. H. Townes, and B. P. Stoicheff, "Stimulated Brillouin scattering and coherent generation of intense hypersonic waves," *Phys. Rev. Lett.* **12**, 592 (1964).
4. G. P. Agrawal, *Nonlinear fiber optics* (Academic, 5th edition, 2012).
5. I. V. Kabakova, R. Pant, D.-Y. Choi, S. Debbarma, B. Luther-Davies, S. J. Madden, and B. J. Eggleton, "Narrow linewidth Brillouin laser based on chalcogenide photonic chip," *Opt. Lett.* **38**, 3208–3211 (2013).
6. K. Hu, I. V. Kabakova, T. F. S. Büttner, S. Lefrancois, D. D. Hudson, S. He, and B. J. Eggleton, "Low-threshold Brillouin laser at 2 μ m based on suspended-core chalcogenide fiber," *Opt. Lett.* **39**, 4651–4654 (2014).
7. X. Huang and S. Fan, "Complete all-optical silica fiber isolator via Stimulated Brillouin Scattering," *J. Lightwave Technol.* **29**, 2267–2275 (2011).
8. B. Morrison, D. Marpaung, R. Pant, E. Li, D.-Y. Choi, S. Madden, B. Luther-Davies, and B. J. Eggleton, "Tunable microwave photonic notch filter using on-chip stimulated Brillouin scattering," *Opt. Commun.* **313**, 85–89 (2014).
9. P. Dainese, P. St. J. Russell, N. Joly, J. C. Knight, G. S. Wiederhecker, H. L. Fragnito, V. Laude, and A. Kheif, "Stimulated Brillouin scattering from multi-GHz-guided acoustic phonons in nanostructured photonic crystal fibres," *Nat. Phys.* **2**, 388–392 (2006).
10. M. S. Kang, A. Nazarkin, A. Brenn, and P. St. J. Russell, "Tightly trapped acoustic phonons in photonic crystal fibres as highly nonlinear artificial Raman oscillators," *Nat. Phys.* **5**, 276–280 (2009).
11. C. Florea, M. Bashkansky, Z. Dutton, J. Sanghera, P. Pureza, and I. Aggarwal, "Stimulated Brillouin scattering in single-mode As₂S₃ and As₂Se₃ chalcogenide fibers," *Opt. Express* **14**, 12063–12070 (2006).
12. H. Shin, W. Qiu, R. Jarecki, J. A. Cox, R. H. Olsson III, A. Starbuck, Z. Wang, and P. T. Rakich, "Tailorable stimulated Brillouin scattering in nanoscale silicon waveguides," *Nat. Comm.* **4**, 1944 (2013).
13. P. T. Rakich, P. Davids, and Z. Wang, "Tailoring optical forces in waveguides through radiation pressure and electrostrictive forces," *Opt. Express* **18**, 14439–14453 (2010).
14. P. T. Rakich, C. Reinke, R. Camacho, P. Davids, and Z. Wang, "Giant enhancement of stimulated Brillouin scattering in the subwavelength Limit," *Phys. Rev. X* **2**, 011008 (2012).

15. R. Pant, C. G. Poulton, D.-Y. Choi, H. Mcfarlane, S. Hile, E. Li, L. Thévenaz, B. Luther-Davies, S. J. Madden, and B. J. Eggleton, "On-chip stimulated Brillouin scattering," *Opt. Express* **19**, 8285–8290 (2011).
 16. C. Wolff, M. J. Steel, B. J. Eggleton, and C. G. Poulton, "Stimulated Brillouin Scattering in integrated photonic waveguides: forces, scattering mechanisms and coupled mode analysis," *arXiv:1407.3521 [physics.optics]*, (2014).
 17. W. Qiu, P. T. Rakich, H. Shin, H. Dong, M. Solja, and Z. Wang, "Stimulated Brillouin scattering in nanoscale silicon step-index waveguides: a general framework of selection rules and calculating SBS gain," *Opt. Express* **21**, 31402–31419 (2013).
 18. P. R. McIsaac, "Symmetry-Induced Modal Characteristics of Uniform Waveguides - I: Summary of Results," *IEEE Trans. Microw. Theory Tech.* **23**, 421–429 (1975).
 19. P. R. McIsaac, "Symmetry-Induced Modal Characteristics of Uniform Waveguides - IT: Theory," *IEEE Trans. Microw. Theory Tech.* **23**, 429–433 (1975).
 20. J. M. Hollas, *Modern spectroscopy* (Wiley, 4th edition, 2004).
 21. D. F. Nelson and M. Lax, "Theory of the Photoelastic Interaction," *Phys. Rev. B* **3**, 2778 (1971).
 22. M. Lax, *Symmetry Principles in Solid State and Molecular Physics*, (Dover Publications Inc., 1974).
 23. M. S. Dresselhaus, G. Dresselhaus and A. Jorio, *Group Theory: Application to the Physics of Condensed Matter*, (Springer, 2008).
 24. I. M. Bassett and A. Argyros, "Elimination of polarization degeneracy in round waveguides," *Optics Express*, **10**, 1342–1346 (2002).
 25. C. M. de Sterke, I. M. Bassett, and A. G. Street, "Differential losses in Bragg fibers," *J. Appl. Phys.* **76**, 680–688 (1994).
-

1. Introduction

Stimulated Brillouin Scattering (SBS) is the coherent nonlinear interaction between light and sound in matter [1]. It was initially predicted by Brillouin [2] and subsequently observed in quartz shortly after the invention of the laser [3]. It is a third-order nonlinear process with several technological applications. Under suitable conditions including narrow pump sources, the effect can be very strong—it has the lowest threshold of all nonlinear processes in standard optical fibres [4]. Still, long interaction lengths are usually required to obtain appreciable interaction at moderate light intensities. As a result, most existing or proposed applications such as Brillouin lasers [5, 6], all-optical isolators [7] or in microwave photonics [8] are based on optical fibers or on-chip waveguides. The interaction in conventional fibers is dominated by electrostriction and the photoelastic effect, which, until relatively recently, were viewed as the only significant processes underlying SBS.

Due to the nonlinear nature of the process, however, the interaction can be dramatically increased in strength by confining the optical mode more tightly, thereby increasing the field intensity for the same transmitted power. Consequently, theoretical and experimental investigations of SBS in structured fibers and integrated photonic waveguides have recently received considerable attention [9–15] with new physical mechanisms [13, 14, 16] being found to contribute to the SBS gain. In addition to the intensity enhancement, such structured waveguides further differ from traditional systems such as step-index fibers in that they support a broad variety of acoustic and optical modes. As solutions to linear wave equations, both sets of modes must respect the waveguide's symmetries (rectangular for many integrated waveguides, triangular or hexagonal for many photonic crystal or suspended core fibers), as expressed by their corresponding point groups. These symmetries play a key role in the question of whether a given combination of optical and acoustic modes can have non-zero SBS-interaction. This fact has been recently studied for the specific case of a rectangular waveguide; Qiu et al. [17] numerically computed SBS gains for a range of possible interactions and found starkly different gains for different mode combinations.

In this paper, we approach SBS interactions on a formal level using group representation theory. We derive clear selection rules for SBS in rectangular, triangular and hexagonal waveguides, these being the most common point-groups arising in photonic waveguides. Although the formalism of group theory is a well-established approach in studying physical interactions of all types, its use in multi-wave interactions in the context of photonic waveguides has been

relatively limited. The definitive categorization of symmetry classes for optical modes was given by McIsaac [18, 19], however the acoustic modes have not been similarly analyzed, and a systematic tabulation of the different types of acoustic modes, including their symmetries and possible degeneracies, is one aim of the present study. More importantly, SBS involves interactions between optical and acoustic modes in nonlinear combination, and the correct conjunction of modes that will permit a non-zero contribution to the gain is a non-trivial problem. Here, we systematically show which acoustic modes can be used to drive SBS transitions between optical modes, and conversely, which optical modes can be used to generate desired acoustic vibrations.

To help motivate our treatment, we note that SBS in structured waveguides is an unusually complex nonlinear interaction, because of the complicated nature of the acoustic dispersion relation which features many modes of different symmetry at moderate acoustic frequencies. In contrast, for SBS in step index fibers, only one acoustic mode is relevant, while for other nonlinearities, acoustic modes of course do not enter at all. In contrast to the optical modes (which can be seeded if necessary), there is limited direct control over the type of acoustic mode that is excited due to the small acoustic propagation length. Instead, the active acoustic mode is selected by the waveguide’s geometry and the symmetry properties of the optical modes. While brute-force computations of coupling integrals are always an option, a refined knowledge of this interplay of the modes’ and the waveguide’s symmetries can be of great value in disentangling the acousto-optic coupling dynamics in complex geometries. It can also indicate which symmetries (or perhaps near symmetries,) of a system are responsible for an unfavorably small or strong coupling. As an indication of its potential power, the symmetry analysis of SBS is analogous to the situation in Raman molecular spectroscopy [20], where the the symmetry properties of the molecule under study determine the presence or absence of a given resonant line for given input and output polarization. Indeed, the relevant overlap integrals (see below) have rather similar forms.

Our selection rules give important physical insight into the dominant couplings in SBS-active experiments, and can be used to greatly reduce the number of mode combinations that have to be considered in gain calculations. For example, we show that for backwards SBS, which generally involves transitions between the same optical mode, no flexural or torsional acoustic modes can possibly contribute to the gain in rectangular or hexagonal structures, whereas flexural modes can contribute in triangular waveguides. Knowledge of the appropriate symmetries of the acoustic modes can also simplify the design of SBS-active waveguides, because once the symmetries of the interacting modes are known, the computational domains can be restricted by imposing appropriate boundary conditions along planes of high symmetry [18]. This of course significantly reduces the calculation time, but more importantly it greatly simplifies the isolation of degenerate or near-degenerate modes.

The paper is organized as follows: In Sections 2 we recall some key results about opto-acoustic coupling in SBS processes. In Section 3, we briefly review the relevant fundamentals of group representation theory. In Section 4, we formulate the acousto-optic interaction in a way that is convenient for a symmetry analysis, and thereby derive a necessary condition on the mode symmetries to permit non-zero SBS-gain. Up to this point, the paper applies to any waveguide symmetry, including circular waveguides and more exotic cases such as five-fold symmetry. In Section 5, we apply this to the aforementioned three important symmetry classes (rectangular, triangular, hexagonal) and provide examples for combinations of modes with non-vanishing interaction. Section 6 concludes our paper.

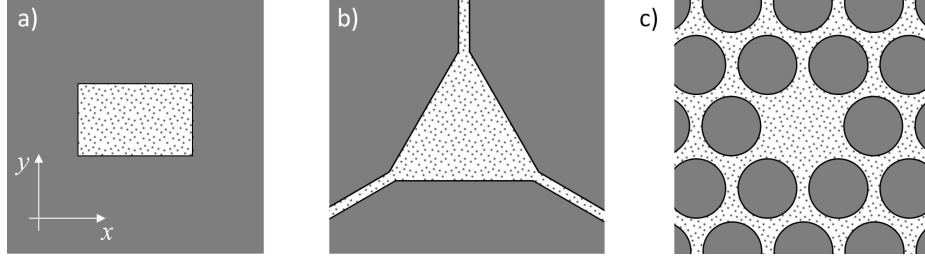


Fig. 1. Illustration of three different waveguide groups, divided according to the waveguide symmetry; a) rectangular waveguides (\mathcal{C}_{2v} group), b) triangular waveguides (\mathcal{C}_{3v} group) and c) hexagonal waveguides (\mathcal{C}_{6v} group).

2. Opto-acoustic coupling in SBS

We consider longitudinally invariant opto-acoustic waveguides oriented along the z -axis, and possessing some degree of rotation or reflection symmetry in the x - y -plane (see Fig. 1). The SBS process can be described either in terms of field perturbations or in terms of optical forces and the mechanical displacement field. The descriptions are equivalent [16]; here we choose to work with the optical forces. The coupling between optical and acoustic modes is proportional to the overlap integral

$$Q = \int d^2r \mathbf{u}^*(\mathbf{r}) \cdot \mathbf{f}(\mathbf{r}) = \int d^2r w(\mathbf{r}), \quad (1)$$

where \mathbf{u} is the displacement field pattern of the relevant acoustic mode and \mathbf{f} is the contribution of the optical force field (due to the two interacting optical modes) that is phase-matched to the acoustic mode. The integration is carried out over the cross section of the waveguide. Most key properties of the SBS interaction follow from knowledge of Q . For example, in long waveguides at steady state, the conventional SBS power gain parameter Γ is given by

$$\Gamma = \frac{2\omega\Omega|Q|^2}{\mathcal{P}^3} \Re \left\{ \frac{1}{\alpha - i\kappa} \right\}, \quad (2)$$

where κ is a detuning from phase-matching, α is the attenuation coefficient of the phonon mode, and the optical and acoustic modes have been assumed to carry one unit \mathcal{P} of power. Thus, maximizing the efficiency of calculation and understanding of the overlap Q underlies effective manipulation of SBS as a nonlinear tool.

As discussed in a number of recent works [13, 14, 16] the force field \mathbf{f} has two contributions: electrostriction and boundary radiation pressure, which lead to separate contributions to the coupling density

$$w(\mathbf{r}) = \underbrace{\varepsilon_0 [\varepsilon_r(\mathbf{r})]^2 \sum_{ijkl} p_{ijkl}(\mathbf{r}) [e_i^{(1)}]^* e_j^{(2)} \partial_k u_l^*}_{\text{electrostriction}} + \underbrace{\varepsilon_0 (\varepsilon_r^{(a)} - \varepsilon_r^{(b)}) \sum_{ijkl} M_{ijkl} [e_i^{(1)}]^* e_j^{(2)} n_k u_l^*}_{\text{radiation pressure}}. \quad (3)$$

In the first term, which describes electrostriction, ε_0 is the permittivity of free space, $\varepsilon_r(\mathbf{r})$ and $\mathbf{p}(\mathbf{r})$ are the local relative dielectric constant and fourth rank photoelastic tensor, and $\mathbf{e}^{(1,2)}$ are the complex mode amplitudes of the two optical fields. The second term, describing radiation pressure, is expressed in terms of field value limits on the interior waveguide boundary through the waveguide local normal vector \mathbf{n} , the dielectric constants $\varepsilon_r^{(a,b)}$ of the core (a) and cladding

Table 1. Relevant parts of the character tables for the groups \mathcal{C}_{2v} , \mathcal{C}_{3v} and \mathcal{C}_{6v} . These tables are standard in many textbooks on group theory and we reproduce them here for convenience following the notation of [22].

\mathcal{C}_{2v}	E	C_2	σ_y	σ_x	\mathcal{C}_{3v}	E	C_3	σ_x	\mathcal{C}_{6v}	E	$2C_3$	$3\sigma_y$	C_2	$2C_6$	$3\sigma_x$
A	1	1	1	1	A_1	1	1	1	A_1	1	1	1	1	1	1
B_1	1	-1	1	-1	A_2	1	1	-1	A_2	1	1	-1	1	1	-1
B_2	1	1	-1	-1	E	2	-1	0	B_1	1	1	1	-1	-1	-1
B_3	1	-1	-1	1					B_2	1	1	-1	-1	-1	1
									E_1	2	-1	0	-2	1	0
									E_2	2	-1	0	2	-1	0

(b) media and the fully invariant tensor [13, 16]

$$M_{ijkl}(\mathbf{r}) = \left[(1 - \delta_{ik})(1 - \delta_{jk}) - \frac{\epsilon_r^{(a)}}{\epsilon_r^{(b)}} \delta_{ik} \delta_{jk} \right] \delta_{kl} \delta(\mathbf{r} \in \mathcal{B}) = M_{jikl} = M_{klij}. \quad (4)$$

Here δ_{ij} is the Kronecker symbol and $\delta(\mathbf{r} \in \mathcal{B})$ is a slightly simplified notation for the Dirac distribution of a function that has its zeros on the boundaries \mathcal{B} between different dielectrics. This distribution $\delta(\mathbf{r} \in \mathcal{B})$ expresses the fact that radiation pressure is confined to the material interfaces. More technically, it is required in order to formulate the more naturally arising contour integral in the form of the area integral in Eq. (3). A third term is caused by the interaction between the magnetic optical fields and a dynamic magnetization caused by the motion of the material [16]. This term can be effectively treated as an antisymmetric part of the photoelastic tensor \mathbf{p} [21] and is typically weak.

The primary goal of this paper is to use symmetry arguments to provide a systematic and efficient procedure for determining whether the integral in Eq. (1) is non-vanishing or not.

3. Symmetry properties of optical and acoustic modes

To proceed, we must recall a number of properties of the representation theory of discrete point groups (see for example [22, 23]). Formally, let \hat{R} be a point symmetry operator, i.e. a rotation or mirror operation about the (longitudinal) z -axis, and let \mathcal{R} be the corresponding 3×3 -matrix that performs this operation in Cartesian space. The image of a scalar function $\phi(\mathbf{r})$ under \hat{R} is found by transforming the underlying coordinate system $\mathbf{r} = (x, y, z)$:

$$\hat{R}\phi(\mathbf{r}) = \phi(\mathcal{R}^{-1}\mathbf{r}). \quad (5)$$

If the function is vector or tensor-valued, these values must also be transformed. For a first rank tensor (i.e. vector) field $\mathbf{v}(\mathbf{r})$ (such as the electric field or the mechanical displacement field) and a second rank tensor field $\mathbf{T}(\mathbf{r})$ (e.g. the stress tensor) the transformation becomes:

$$[\hat{R}\mathbf{v}(\mathbf{r})]_i = \sum_j v_j(\mathcal{R}^{-1}\mathbf{r}) \mathcal{R}_{ji}; \quad [\hat{R}\mathbf{T}(\mathbf{r})]_{ij} = \sum_{kl} T_{kl}(\mathcal{R}^{-1}\mathbf{r}) \mathcal{R}_{ki} \mathcal{R}_{lj}. \quad (6)$$

Pseudotensorial quantities such as the magnetic field differ from this transformation by an additional factor $\det \mathcal{R} = \pm 1$.

If the waveguide in all its aspects (specifically including its tensorial material parameters,) is invariant with respect to a given set of point symmetry operations, these operations form a group \mathcal{G} with respect to composition. Common examples are the \mathcal{C}_{2v} , \mathcal{C}_{3v} and \mathcal{C}_{6v} groups that apply to waveguides with rectangular, triangular and hexagonal symmetry. The elements of the \mathcal{C}_{nv} groups consist of the identity operation (E), all multiples of the $2\pi/n$ rotation (C_n),

and $2n$ reflection operations that are created by successively applying half the fundamental rotation operation, i.e. by applying the π/n -rotation to the x -mirror operation (σ_x), which maps any vector (x, y, z) to $(-x, y, z)$. For each excitation frequency ω , the set of (optical or acoustic) modes $\{f^{(i)}(\mathbf{r})\}$ with the same wavenumber forms a linear subspace \mathcal{S}_f that is invariant under all operations in \mathcal{G} . Each symmetry operation $\hat{R} \in \mathcal{G}$ can therefore be expressed as an expansion in the basis of the mode functions $f^{(i)}(\mathbf{r})$:

$$\hat{R}f^{(i)} = \sum_j f^{(j)} \mathcal{D}^{(\hat{R})}_{ji}. \quad (7)$$

In general $\mathcal{D}^{(\hat{R})}$ are matrices, however in the non-degenerate case, in which the set $\{f^{(i)}(\mathbf{r})\}$ consists of a single function, the matrices reduce to scalar phase factors. In the degenerate case, the matrices $\mathcal{D}^{(\hat{R})}$ depend on the choice of basis functions $f^{(i)}(\mathbf{r})$ and are unitary for any ortho-normal basis.

The set of matrices $\mathcal{D}^{(\hat{R})}$ for all elements $\hat{R} \in \mathcal{G}$ is known as a (matrix) *representation* of the underlying symmetry group \mathcal{G} , which means that these matrices fulfill the multiplication rules of the abstract group elements. Different mode types induce specific representations that are associated with the modal symmetry. As the matrices themselves depend on the choice of basis functions, they are ill-suited to characterize the symmetry of a degenerate subspace. Instead, the natural choice are the matrices' traces, which are invariant under similarity transformations and called the *characters* of the representation matrices. For a non-degenerate mode that is even with respect to all elements $\hat{R} \in \mathcal{G}$, that is, it is unchanged under all operations in the group, the representation induced by the mode consists of $\mathcal{D}^{(\hat{R})} = 1$ for each element \hat{R} . This trivial representation, denoted by A or by A_1 exists for each group and corresponds to monopole-like fields. We should stress that the mere existence of this representation does not mean that the (optical or acoustic) wave equation will necessarily have a physical solution of this symmetry at any given frequency (indeed the fundamental mode of a dielectric waveguide is only rarely of A_1 type [24, 25]). Representations that are characterized by sign changes under the various operations of the group (rotations and reflections) correspond to higher-order multipole fields or superpositions thereof and are denoted A_2 , B -type or E -type representations, the latter denoting degenerate representations. Table 1 lists the characters of all irreducible representations of the three point groups under consideration, for sets of operations that are sufficient to unambiguously identify the representations based on their characters. These tables are reproduced from [22] (and found in many other texts). The degenerate representations E and E_1 of the groups \mathcal{C}_{3v} and \mathcal{C}_{6v} , respectively, are particularly important since the fundamental optical mode of a dielectric waveguide with threefold or sixfold symmetry is of this type in practical situations involving index-guided waveguides.

The acousto-optic overlap integral involves a product of three modes (two optical and one acoustic), so we need the symmetry properties of products. The product of two modes $f^{(i)}(\mathbf{r}) \cdot g^{(j)}(\mathbf{r})$ from two invariant subspaces \mathcal{S}_f and \mathcal{S}_g lies inside the direct product subspace spanned by every possible product $\mathcal{S}_f \otimes \mathcal{S}_g = \text{span}\{f^{(i)}(\mathbf{r})g^{(j)}(\mathbf{r})\}$. If \mathcal{S}_f is one-dimensional, the characters of $\mathcal{S}_f \otimes \mathcal{S}_g$ are obtained by simply multiplying the characters of \mathcal{S}_g with those of \mathcal{S}_f (and analogously if \mathcal{S}_g is one-dimensional). If both subspaces are degenerate (with dimensions n and m), the product space is $n \times m$ -dimensional and usually reducible into the few irreducible representations of the point group, i.e. it can be decomposed into a number of independent smaller subspaces. In the context of discrete symmetry groups for waveguides, this is always the case. The details of this decomposition depend on whether $\mathcal{S}_f \neq \mathcal{S}_g$ (general case), or whether the functions $f^{(i)}(\mathbf{r})$ and $g^{(j)}(\mathbf{r})$ are identical or orthogonal to each other within the same degenerate subspace $\mathcal{S}_f = \mathcal{S}_g$. Within the context of SBS, the latter appears if the two optical modes have (up to the Stokes shift) the same frequency and wave number. "Identi-

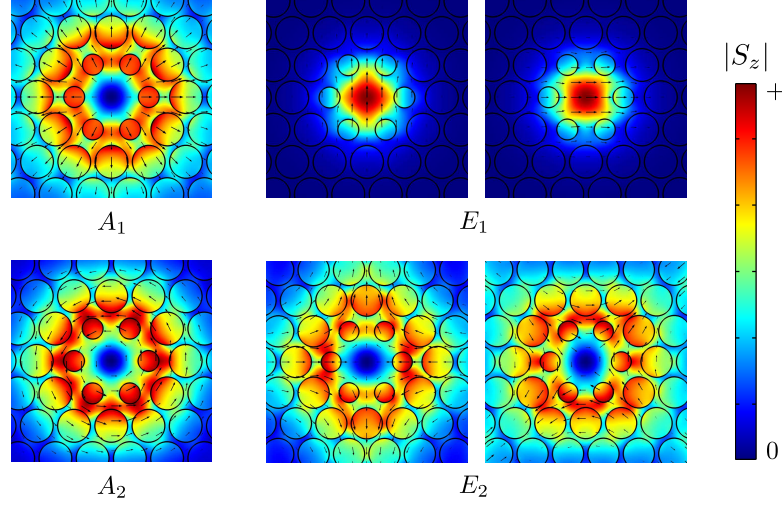


Fig. 2. Electric field patterns for the fundamental optical modes in a structured silica fiber with hexagonal symmetry. The arrows represent the transversal field components. The color represents the time-averaged power density directed along the waveguide axis (i.e. the z -component of the time-averaged Poynting vector). The color scale is in arbitrary units.

cal” in this context means that the optical mode is red-shifted in frequency but its polarization state is not affected. “Orthogonal” refers for example to the case that the polarization state is completely changed, i.e. that the source and destination states are orthogonal. The general rule applies whenever one of the involved modes has a degenerate partner that is not excited by the SBS-process under consideration. For example, the flexural acoustic modes in \mathcal{C}_{3v} or \mathcal{C}_{6v} systems always appear in pairs, even though only one of these mode may contribute in a specific setup.

For the two point groups under consideration that feature degenerate representations, the product decompositions are listed in Table 2. Again, these tables are reproduced from [22].

3.1 Examples for optical and acoustic modes

The symmetry properties of optical waveguides are well-known [18]. Here we show some specific examples to illustrate how the group-theoretical representation relates to the more widely-used categories of waveguide modes. In Fig. 2 we show examples of optical modes of a photonic crystal fiber, with a structure belonging to the \mathcal{C}_{6v} point group. The two fundamental modes have E_1 -symmetry, and correspond to the fundamental linearly x - and y -polarized modes (often classified as HE_{11} modes, by way of analogy with the step-index fiber). These modes are the most relevant for optical experiments, since they are readily coupled into from free space or other waveguides. Higher order modes are also possible in this structure; in this specific configuration and at this frequency these are all cladding modes, however these mode types can become important for large-core structures. The first higher-order x and y polarized modes are of E_2 type and are also degenerate. The A_1 type mode in Fig. 2 has an electric field pointing radially outward, this mode possessing even vectorial symmetry both under all reflections and rotations, in accordance with Table 1. The A_2 -type mode has odd symmetry under all reflections and even symmetry under all rotations; this “donut” mode rotates its polarization with respect to angle and possess a phase singularity at the origin, and is analogous to the TE_{01} mode of the step-index fiber. The B_1 and B_2 type modes arise rarely in practical situations and so we have omitted these in the figure; a sketch of the properties of these modes can be found in Fig. 5. In

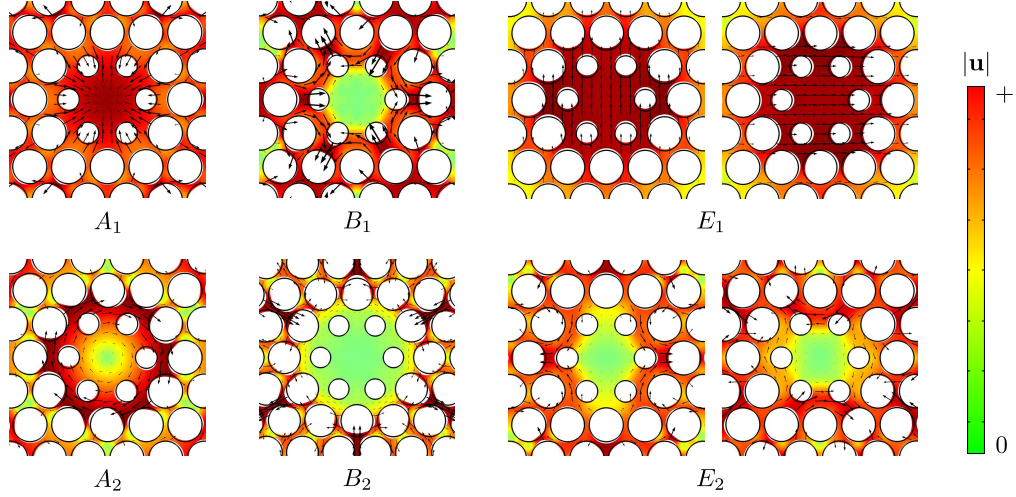


Fig. 3. Examples for the symmetries of acoustic modes in a structured silica fiber with hexagonal symmetry. The arrows and the deformation plot indicate the in-plane components $\mathbf{u}_\perp = (u_x, u_y, 0)$ of the mechanical displacement field. The color represents the absolute value of the total displacement field $|\mathbf{u}| = \sqrt{|u_x|^2 + |u_y|^2 + |u_z|^2}$. The color scale is in arbitrary units.

all cases we note that it is the transformation properties of the electric field which determine the classification, the magnetic field being a pseudo-vector.

The symmetry properties of acoustic modes are perhaps less known within the photonics community. In Fig. 3 we show examples of the different types of acoustic modes, again for the \mathcal{C}_{6v} point group. The A_1 type mode corresponds to a longitudinal-like acoustic mode, because the dominant motion is in the waveguide direction. The A_2 -type mode is a torsional-like mode, and the degenerate pair of E_1 modes are the orthogonally-polarized fundamental flexural modes. The additional degenerate pair of E_2 -type acoustic modes either stretches or shears the core in the horizontal direction, rather than displacing the core as a whole. This representation covers e.g. accordion-like “breathing modes”, which simultaneously stretch the core horizontally while compressing it vertically. The acoustic B_1 and B_2 modes describe non-degenerate higher-order vibrations. The B_1 modes displace the material either inwards or outwards along symmetry planes separated by 120 degrees, while displacing material in the opposite direction along the alternate symmetry planes. The B_2 modes act in a similar way to the B_1 modes, but with the symmetry planes rotated by 30 degrees.

4. Formal selection rule

The term “selection rule” usually refers to a set of constraints on the symmetry properties of physical states to allow for interaction. The best known example of these are the conditions for the atomic states between which optical transitions can occur. For that problem, the point group is the group of continuous rotations and the irreducible representations are distinguished by the two angular momentum quantum numbers. Transitions can occur if the product of the two electronic representations and the representation decomposition of the electric dipole operator has a trivial (i.e. with total angular momentum $L = 0$) contribution, which is just another formulation of the well known optical selection rules $\Delta L = \pm 1$ and $-1 \leq \Delta m \leq 1$. Similar rules for discrete symmetry groups of atoms in solids are known from the context of crystal field theory.

In this section, we formulate the problem of acousto-optic interaction in a very similar picture, where the optical waveguide modes are analogous to the electronic eigenstates and the

Table 2. Relevant parts of the product decomposition tables for \mathcal{C}_{3v} and \mathcal{C}_{6v} . The abbreviations “i.d.m.” and “o.d.m.” in the decomposition tables stand for “identical degenerate modes” and “orthogonal degenerate modes”, respectively. See Section 3. for details. Again, these tables are standard in many textbooks on group theory such as [22].

Product decomposition for \mathcal{C}_{3v}		Product decomposition for \mathcal{C}_{6v}	
$E \otimes E = A_1 \oplus E$	(i.d.m.)	$E_1 \otimes E_1 = A_1 \oplus E_2$	(i.d.m.)
$E \otimes E = A_2$	(o.d.m.)	$E_1 \otimes E_1 = A_2$	(o.d.m.)
$E \otimes E = A_1 \oplus A_2 \oplus E$	(general)	$E_1 \otimes E_1 = A_1 \oplus A_2 \oplus E_2$	(general)
		$E_2 \otimes E_2 = A_1 \oplus E_2$	(i.d.m.)
		$E_2 \otimes E_2 = A_2$	(o.d.m.)
		$E_2 \otimes E_2 = A_1 \oplus A_2 \oplus E_2$	(general)
		$E_1 \otimes E_2 = B_1 \oplus B_2 \oplus E_1$	(general)

acoustic wave corresponds to the electric dipole operator. Using this, we formulate the opto-acoustic selection rule in its most general form in analogy to the problem of optical transitions in atoms. To this end, we now analyse the symmetry properties of the overlap integral Eq. (3). The photoelastic tensor \mathbf{p} is invariant under the symmetry operations, because we assumed the waveguide (including all material parameters) to be so. This is strictly true for cubic materials in rectangular geometries and for isotropic materials such as silica or various glasses under all circumstances. The tensor \mathbf{M} is invariant by construction. The partial derivative and the normal vector distribution \mathbf{n} induce the trivial group representations. Thus, we can formally write Eq. (3) in the form

$$w = \sum_{ijk} N_{ijk} [e_i^{(1)}]^* e_j^{(2)} u_k^*, \quad (8)$$

where the third rank tensor operator \mathbf{N} is invariant under all waveguide symmetries, and induces the trivial representation A or A_1 , depending on the precise group.

To formulate the selection rule for SBS, we first write the integrand as the superposition of symmetric functions $w = \sum_{\alpha} w_{\alpha}$, where each index α corresponds to one irreducible representation. The integrals over all symmetric contributions are zero except for the trivial representation [22]. That is, the coupling integral Q can be only non-zero for modes whose product contains the trivial representation (note however that this does not imply that the integral over a trivial representation is always non-zero). To this end, we first determine the symmetry properties of the product between the two optical modes, either by simply multiplying the characters from Table 1 in the case of at least one non-degenerate mode or by using Table 2 if both modes are degenerate. In the same way, we then combine every irreducible representation from this first product with the acoustic representation. If this yields a trivial representation, coupling is possible.

To illustrate this evaluation of representation products, we give two examples: First assume that in a rectangular waveguide the optical representations are B_1 and B_3 and the acoustic representation is also B_3 . The product of the characters of B_1 and B_3 result in the characters of B_2 , thus the product of the two optical modes has B_2 -symmetry. The product of these characters and those of the acoustic B_3 -representation indicate that the product of all three modes has B_1 -symmetry, and hence that the overlap integral vanishes.

Second, assume that in a hexagonal waveguide the optical representations are E_1 and E_2 and the acoustic representation is B_1 . From Table 2 we can see that the product of the optical modes is a superposition of a B_1 -, a B_2 - and a degenerate E_1 -representation. Each of these represen-

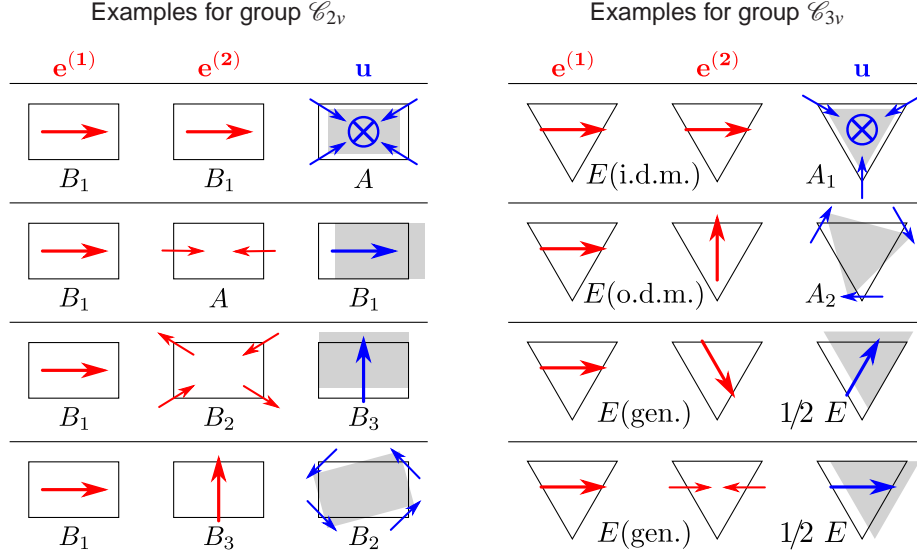


Fig. 4. Typical examples for combinations of symmetric eigenmodes that can have non-zero opto-acoustic overlap for the point groups \mathcal{C}_{2v} (left hand side) and \mathcal{C}_{3v} (right hand side). Each line contains sketches of two optical modes (left and middle column) and one acoustic mode (right column). The symmetry of the undistorted waveguide is represented by a black polygon, the effect of distortion is sketched in light gray. Red arrows indicate the general behavior of the major component of the optical modes' electric fields. Blue arrows indicate the general behavior of the acoustic displacement field.

tations are now individually combined with the acoustic B_1 -representation to find the decomposition of the total integrand: it is a superposition of an A_1 -, an A_2 - and an E_2 -representation. The integral over the latter two contributions vanishes, but the integral over the first term can be non-zero. Thus coupling is possible but may depend on the exact choice of the optical modes within their respective E_1 - and E_2 -subspaces.

5. Examples for SBS-active mode combinations

We now examine the three most important cases in more detail.

5.1 Rectangular group \mathcal{C}_{2v}

The rectangular group does not exhibit any degenerate representations and is therefore simple to discuss. The symmetry of the integrand in Eq. (8) can be easily established by multiplying the characters of the constituent representations. We find two classes of combinations that lead to w having trivial symmetry. The first class is if two modes have identical symmetry and the third one has A -symmetry. This is the case in backward SBS, where the two optical modes have identical symmetry (but opposite propagation direction) and is only possible with an acoustic mode of A -type, i.e. not with flexural or torsional modes. Another example for this class is the conversion between a fundamental, linearly polarized optical mode (B_1 -type or B_3 -type) and a higher order mode (A -type). In this case, the acoustic mode must be of flexural type. The second class is if the optical and acoustic modes cover all three non-trivial representations. This is for example the case for conversion between orthogonally polarized fundamental optical modes (B_1 -type and B_3 -type) and is only possible with an acoustic mode of B_2 -type, i.e. a torsional mode. These combinations are sketched in the left hand part of Fig. 4.

5.2 Triangular group \mathcal{C}_{3v}

The triangular point group supports one degenerate and two non-degenerate representations. The degenerate representations describe linearly polarized optical and flexural acoustic modes. This degeneracy slightly complicates the problem of identifying gain combinations. The reason for this is that the symmetry of the product of degenerate modes depends on the degree of overlap between them. To resolve this, we have to treat the cases of orthogonal eigenmodes (orthogonal polarizations) separately from the case where the two modes have maximally possible overlap (identical polarization). The product decomposition table for the group \mathcal{C}_{3v} in Table 2 shows that the former case always results in a mode of A_2 -symmetry, whereas the latter case leads to a superposition of a trivial and a degenerate representation. The general case of partially overlapping eigenmodes (skew polarizations) is a superposition of these special cases. The same holds if both relevant eigenmodes stem from different degenerate subspaces (e.g. an optical and an acoustic mode of E -symmetry).

As before, we find two classes of gain-supporting combinations. The first case is again the combination of one A_1 -type eigenmodes and two other modes of identical symmetry properties, i.e. either two modes of the same non-degenerate type or a pair of degenerate modes with the same polarization. Again, this implies that backward-SBS requires an A_1 -type, i.e. a longitudinal acoustic mode. The second case is again a combination of all three non-trivial symmetry properties, i.e. one A_2 -type mode and two orthogonal modes of E -type. As in the rectangular case, this means that SBS between orthogonally polarized optical modes requires a torsional mode. The product between a fundamental optical mode and a flexural acoustic mode is the general case of the product decomposition and may contain any representation. This means that a flexural acoustic mode can cause SBS between a fundamental mode and any other optical band, not only between the fundamental and the corresponding higher-order mode. We provide some examples for combinations of modes with non-zero overlap in the right hand part of Fig. 4.

5.3 Hexagonal group \mathcal{C}_{6v}

The hexagonal group \mathcal{C}_{6v} is a supergroup of both \mathcal{C}_{2v} and \mathcal{C}_{3v} , and supports two degenerate and four non-degenerate representations. They emerge from the representations of the \mathcal{C}_{3v} group by including the C_2 operation as a new generator. The E_1 representations include linear polarized (dipole-like) modes, which are the fundamental modes in the optical case. The modes with E_2 symmetry have quadrupolar character, as can be seen in the second-order optical mode provided this is above cut-off (see Fig. 2). The B_1 and B_2 modes have hexapolar character—in contrast to the dipolar and quadrupolar modes these modes are not degenerate—and the A_2 representation correspond to modes with dodecapolar symmetry such as torsional modes in the acoustic case and azimuthally polarized optical modes. As in the rectangular and triangular cases, the A_1 representation corresponds to longitudinal or breathing acoustic modes and radially polarized optical modes.

The analysis of possible gain combinations is greatly simplified by the prior discussion of the two subgroups \mathcal{C}_{2v} and \mathcal{C}_{3v} . First we note that the character table for the non-degenerate representation is very similar to that of \mathcal{C}_{2v} . The only difference are the rotation operators C_3 and C_6 , whose characters are identical to those of E and C_2 in the non-degenerate case. As a consequence, the discussion of Section 5.1 applies to the gain combinations of any non-degenerate representations. Furthermore we notice that the representation table reduces to two separate instances of the \mathcal{C}_{3v} table, which differ only by the sign of the character of the C_2 rotation. As a consequence the discussion of Section 5.2 applies, with the additional constraint that the number of representations that contain a negative character for C_2 must be even in order to obtain the trivial representation.

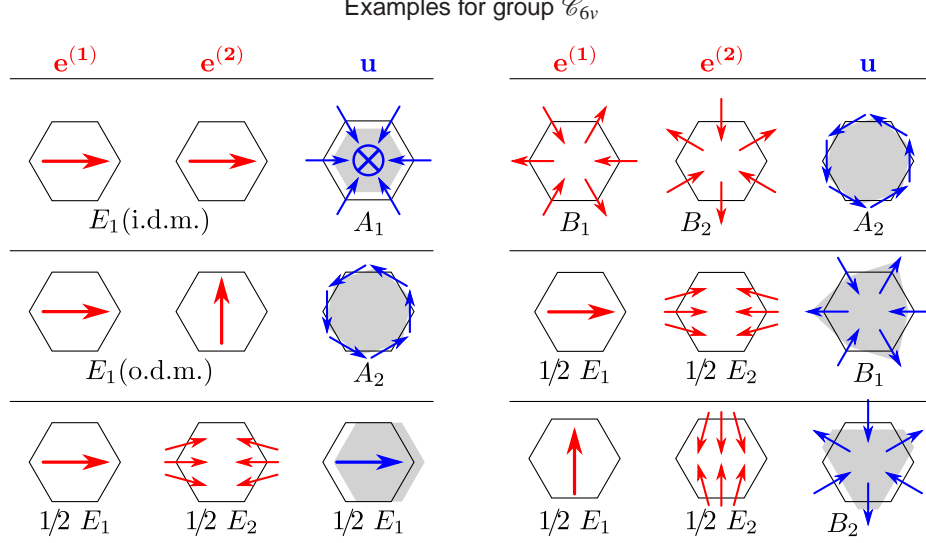


Fig. 5. Typical examples for combinations of symmetric eigenmodes that can have non-zero opto-acoustic overlap for the point group \mathcal{C}_{6v} . See the caption of Fig. 4 for a more detailed description of what is shown here.

The final case is unique to hexagonal structures, and consists of combinations of E_1 together with E_2 modes. This type of interaction must be handled with the help of the product decomposition table (see Table 2). According to this table, two such modes can be combined with either a B -type non-degenerate mode or with an E_1 -type mode in order to obtain non-zero gain. As an example, an optical fundamental mode can couple to the corresponding second order mode via an acoustic flexural mode. Alternatively, an acoustic accordion-like acoustic mode can facilitate the coupling between two optical modes of the same type. A complete discussion of all the possible mode combinations would be excessive without being particularly enlightening; a representative selection of examples that might be important is given in Fig. 5.

6. Conclusion

We have formulated the selection rules for SBS for three important waveguide symmetries. If the symmetry is only weakly broken, for example by anisotropy in the mechanical properties induced by the cubic nature of some materials, we can expect these selection rules to hold to a good approximation. If the symmetry is strongly broken, these rules are readily adapted to waveguides with reduced symmetry—for example, the selection rules for rectangular waveguides on a substrate will reduce to the \mathcal{C}_v group, combinations of which will follow the character table with the σ_y and C_2 operations removed.

Apart from its use in the understanding and design of SBS-active waveguides, our results are very useful for the development and testing of numerical tools. Firstly, they provide sets of modes that should not be able to couple for symmetry reasons. This is an excellent way to identify convergence and discretization issues in the evaluation of the coupling integrals. Secondly, they eliminate complete symmetry classes of acoustic solutions for the interaction between any two given optical eigenmodes. These symmetry constraints can be exploited in numerical calculations by reducing the computational domain and imposing appropriate boundary conditions along the mirror planes, thereby greatly reducing the computational effort. This can be significant in automatized design optimization problems or large-scale geometries.

Acknowledgments

We acknowledge financial support of the Australian Research Council via Discovery Grant DP130100832.